ICIC Express Letters ICIC International ©2016 ISSN 1881-803X
Volume **10**, Number **1**, January **2016** pp. 177–184

A NOVEL ULTRASONIC METHOD OF LARGE-DIAMETER PILES DEFECT TYPE DETECTION BASED ON WPD AND PNN

Lixin Zhang[1], Huijian Li[2,*], He Wang[1] and Zhibin Song[1]

[1]Institute of Urban Construction
Hebei Normal University of Science & Technology
No. 360, West Hebei Street, Qinhuangdao 066004, P. R. China
zhang_lx66@163.com

[2]School of Civil Engineering and Mechanics
Yanshan University
No. 438, West Hebei Street, Qinhuangdao 066004, P. R. China
*Corresponding author: ysulhj@163.com

Received June 2015; accepted August 2015

Abstract. *In this paper, a new method, i.e., Velocity Amplitude Energy Method (VAEM) is proposed to overcome the low accuracy and reliability of Traditional Velocity Amplitude Method (TVAM) in the field of defect type detection of large-diameter concrete piles. In the proposed method, an ultrasonic transmission signal is decomposed into a series of sub-signals with the use of Wavelet Packet Decomposition (WPD). Then, a series of energies of these sub-signals, i.e., the energy spectrum of the original signal, is calculated. To enhance achievements, a comprehensive energy vector (CEV) is constructed with the use of its energy spectrum, velocity and average amplitude, which will be acted as the input vector of neural networks. Finally, Probabilistic Neural Networks (PNN) are built to train and identify. To validate achievements of TVAM and VAEM, a number of practical inspection signals from practical projects are employed. Experimental results show that the average identification rates (AIRs) of TVAM and VAEM are 55% and 79% respectively, which indicates that the proposed method achieves much better performances on accuracy and reliability.*
Keywords: Wavelet packet decomposition, PNN, Ultrasonic transmission method, Large-diameter concrete pile, Velocity Amplitude Energy Method, Defect type detection

1. **Introduction.** Currently, large diameter concrete piles are widely used in huge bridges and high buildings. During construction processes, it is sometimes inevitable that there are some quality defects, such as hole, mud-mixing, dreg-sinking, gravel-aggregating and mortar aggregating, due to the imperfection of constructing technologies and operational errors [1]. To avoid quality and safety accidents, some nondestructive testing (NDT) methods are adopted to evaluate the integrity of piles before next step construction. Ultrasonic transmission method is widely used in the field of large-diameter pile testing [2]. In this method, before the foundation construction, a number of acoustic tubes are placed in the pile as the transducer channels, as illustrated in Figure 1.

Before inspection, water is poured into the transducer channels as couplant. Ultrasonic waves are emitted from the emission sensor, then propagate through the concrete material, and at last received by receiving sensor. During this process, the velocity and amplitude of a wave would change because of the influences of the concrete material and defects. Some typical waves are shown in Figure 2.

In Traditional Velocity Amplitude Method (TVAM), defect types are identified only through observing the velocity and amplitude of waves. As seen in Figure 2, the transmission wave is very complicated and difficult to identify, which leads to relative low accuracy and reliability of TVAM. For this reason, TVAM is usually playing a subsidiary rote in practical inspection projects, that is to say, some destructive and costly inspection

(a) $0.6\text{m} \le D < 1\text{m}$ (b) $1\text{m} \le D < 2.5\text{m}$

FIGURE 1. Layout of transducer channels in large-diameter pile

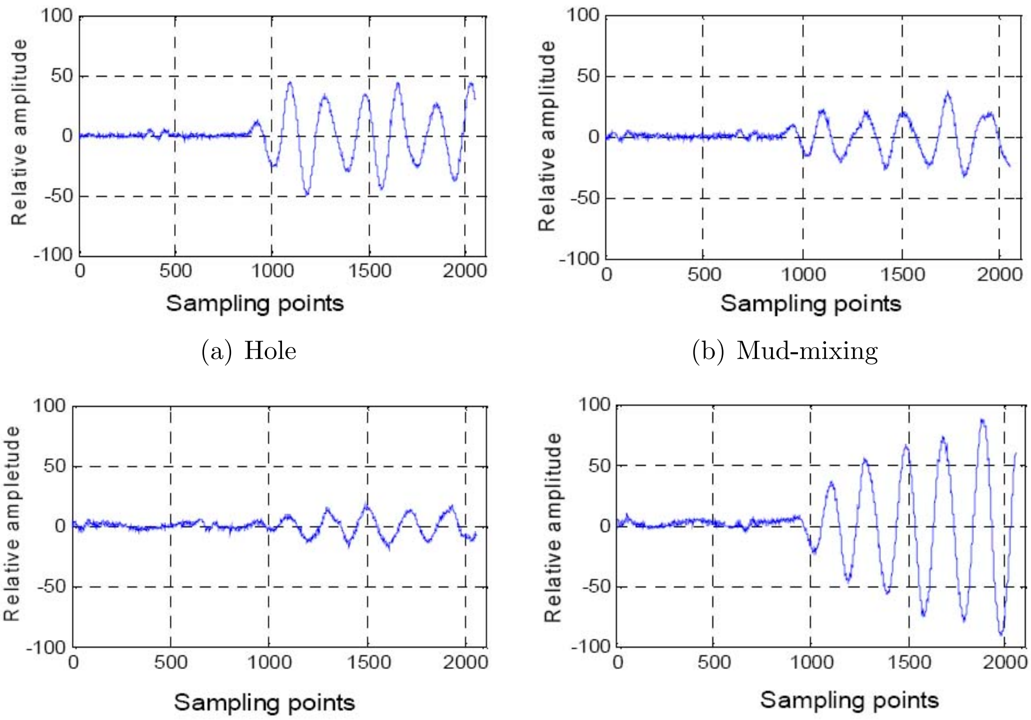

(a) Hole (b) Mud-mixing

(c) Dreg-sinking (d) Gravel-aggregating

FIGURE 2. Typical ultrasonic transmission waves

methods, such as core sampling method and other methods, are usually adopted subsequently to confirm the exact interior status of piles. Hence, a high accuracy and reliability NDT method is urgent.

As we all know, because of different reflection, refraction and absorption at the interfaces of different type defects, the energy attenuations of different frequency bands are different, i.e., different energy spectrums are formed. It should be a feasible way to realize defect type identification. Hence, Velocity Amplitude Energy Method (VAEM) is proposed in this paper.

Wavelet packet decomposition (WPD) is outstanding in feature extraction in recent decades [3,4]. Therefore, in the first stage of VAEM, WPD is adopted to extract the feature energy spectrum from a signal. To enhance classifying performances, some parameters, such as velocity and average amplitude of this signal, are also acquired to construct its comprehensive energy vector (CEV). In the next step, the probabilistic neural network (PNN) is adopted to train and simulate to realize defect type recognition. It should

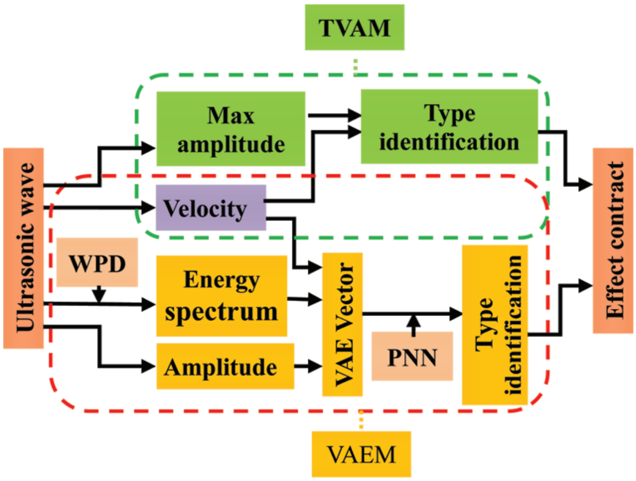

FIGURE 3. Overall flowchart of pile defect type identification

be specially pointed out that the ultrasonic transmission waves utilized in this paper are acquired in practical inspection projects of Qinhuangdao Pile Quality Test Center in recent years. Comparison analysis shows that the average identification rate (AIR) of TVAM is 55%, and that of VAEM is 79%, which demonstrates the obvious advantages of the proposed method. Total identification procedures are shown in Figure 3.

2. WPD and PNN.

2.1. WPD. First a brief introduction of wavelet decomposition is presented. The function $\psi(t)$is a wavelet if it satisfies these two properties:

$$\left.\begin{array}{l}\int_{-\infty}^{+\infty}\psi(t)\mathrm{d}t=0\\ \int_{-\infty}^{+\infty}|\psi(t)|^2\mathrm{d}t<\infty\end{array}\right\} \tag{1}$$

Through translating and scaling, a family waveform can be obtained as

$$\psi_{a,b}(t)=a^{-1/2}\psi\left(\frac{t-b}{a}\right),\quad a>0,\quad b\in R \tag{2}$$

where a and b are the scale parameter and the time parameter respectively [5]. Wavelet decomposition can be expressed as

$$\int_R f(t)\cdot\psi_{a,b}(t)\mathrm{d}t=a^{-1/2}\int_R f(t)\cdot\psi\left(\frac{t-b}{a}\right)\mathrm{d}t \tag{3}$$

Wavelet decomposition has two main properties: multi-resolution or multi-scale analysis in the time-frequency domain and the ability to characterize the local properties of signals in both time and frequency domains. WPD can provide a more sophisticated analysis than wavelet decomposition, because, with multi-level it separates not only the low-frequency part of a signal but also the high-frequency part, which does not do in wavelet decomposition [6]. Furthermore, it can adaptively choose corresponding frequency band to match the signal frequency spectrums based on the feature of a signal. Thereby it can enhance the time-frequency resolution and has more applicable values. Tree of WPD is illustrated in Figure 4, and then the originality signal can be represented as:

$$S=A1+D1=AA2+DA2+AD2+DD2=\cdots \tag{4}$$

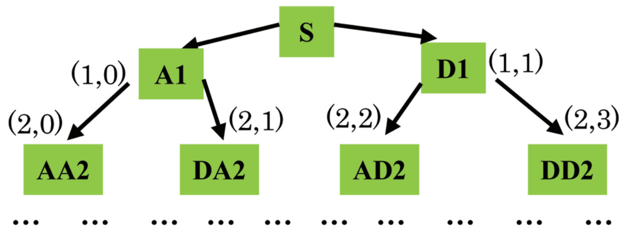

FIGURE 4. The tree of wavelet packet decomposition

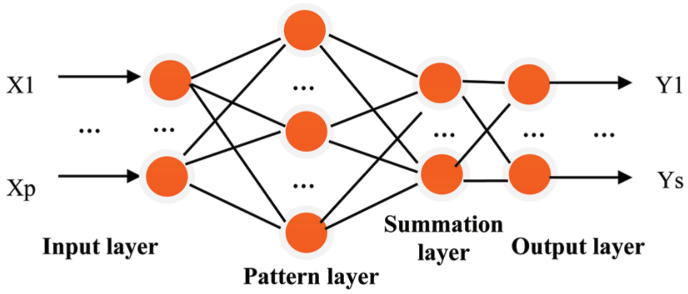

FIGURE 5. Model of PNN

2.2. **PNN.** PNN is a kind of self-monitoring feed forward neural network developed from radial basis function (RBF) network, whose theory basis is the Bayesian minimum risk criteria [7,8]. The PNN model is composed of four layers: the input layer, the pattern layer, the summation layer and the output layer, as shown in Figure 5.

In PNN model, the number of input layer neurons is equal to the number of input vector elements, and the number of output layer is equal to the number of the types of the training samples. Through Equation (5), the output of each unit in the pattern layer is calculated.

$$\Phi_{ij}(x) = (2\pi)^{-0.5d}\sigma^{-d}\exp\left[-\frac{(x-x_{ij})^T(x-x_{ij})}{2\sigma^2}\right] \tag{5}$$

where $i = 1, \cdots, M$, $j = 1, \cdots, N$, M is the total number of classed in the training samples, x_{ij} is the jth mode, N_i is the number of neurons in the pattern layer of the PNN ith class, and σ and d are the smooth parameter and the data dimension of the samples. The summation layer is the cumulative probability belonging to a certain class, which is calculated through Formula (6).

$$f_{iNi}(x) = N_i^{-1}\sum_{j=1}^{N_i}\Phi_{ij}(x) \tag{6}$$

Compared with BP-NN, RBF-NN and other neural networks, PNN has a much faster convergence speed and more powerful classifying ability. Hence, in this paper, it is adopted.

3. **Comprehensive Energy Vector Construction.** In VAEM, the CEV of a signal is constructed with its velocity, average amplitude and energy spectrum. The detailed procedures are follows. Firstly, a wave signal $S(t)$ is decomposed through WPD at m levels, and then a series of sub-signals is obtained, whose number is 2^m. Secondly, a series of energies of these sub-signals is calculated by Formula (7).

$$E_i = \int |S_i(t)|^2 \mathrm{d}t = \sum_{j=1}^{n}|x_{ij}|^2, \ i = 0, 1, \cdots, 2^m; \ \ j = 1, 2, \cdots, n \tag{7}$$

where x_{ij} is the jth amplitude of sub-signal $S_i(t)$. Then the energy spectrum I can be expressed as Equation (8).

$$I = [E_1, E_2, \cdots, E_i], \quad i = 0, 1, \cdots, 2^m \tag{8}$$

The average amplitude AA is calculated through amplitudes of the original signal $S(t)$. Supposing in the original signal, the amplitude of the jth sampling point is x_j, AA of this signal can be defined as Formula (9).

$$AA = \sum_{j=1}^{n} |x_j|, \ \ j = 1, 2, \cdots, n \tag{9}$$

The ultrasonic transmission time is easy to be acquired from the received wave, so the wave velocity V is also easy to be calculated. Suppose the distance between the emission sensor and the receiving sensor is l, the time of the head wave is t, and then $V = l/t$. To be easy to converge with the use of PNNs, all elements of the CEV are processed and turned into relative values. Then the CEV of the wave can be expressed as Equation (10).

$$I = \left[\frac{E_1}{E_{1\max}}, \frac{E_2}{E_{2\max}}, \cdots, \frac{E_i}{E_{i\max}}, \frac{V}{V_{\max}}, \frac{AA}{AA_{\max}}\right] \tag{10}$$

where $E_{1\max}, E_{2\max}, \cdots, E_{i\max}, V_{\max}$ and $AA_{\max}$ are the maximum value among the same kind datum of all sample waves.

4. **Experiment and Valuation.** The entire inspection system diagram is shown in Figure 6. After the emission sensor and the receiving sensor (always on the same elevation) move from the bottom to the top of a pile, the whole pile testing is finished.

4.1. **Defect type detection based on TVAM.** In TVAM, the velocity and amplitude of a wave are acquired first, and common experience identification laws are listed in Table 1.

The ultrasonic waves adopted in this paper are acquired in practical inspection projects, and the exact types of them are confirmed through other inspection approaches. Based

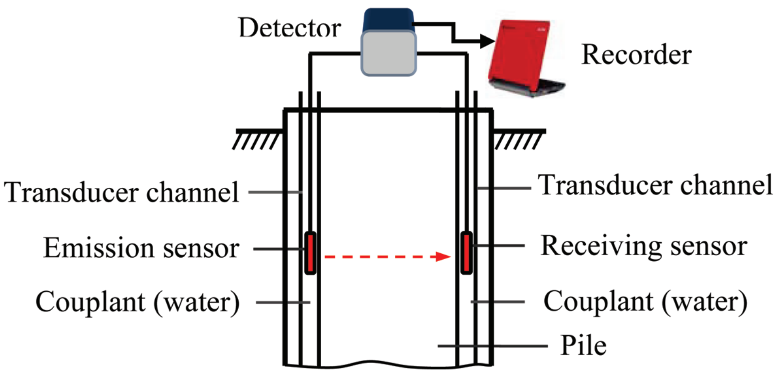

Figure 6. Total inspection system diagram of TVAM

Table 1. Experience laws of defect type identification

Defect type	Hole	Mud -mixing	Dreg -sinking	Gravel -aggregating	Mortar -aggregating
Velocity	Reduce	Reduce significantly	Reduce Sharply	Reduce or not	Reduce
Amplitude	Reduce significantly	Reduce significantly	Reduce Sharply	Reduce	No-change or increase slightly

TABLE 2. Identification results of TVAM

Defect type	Hole	Mud -mixing	Dreg -sinking	Gravel -aggregating	Mortar -aggregating
Total	70	60	50	50	50
Identification	37	34	30	25	27
Identification rate	53%	57%	60%	50%	54%

TABLE 3. Part of CEVs

Defect type		Hole	Mud-fixing	Dreg -sinking	Gravel -aggregating	Mortar -aggregating
$V/V_{\max}$		0.9603	0.9393	0.9206	1.0000	0.9953
$\sum\lvert A_i\rvert/(\sum\lvert A_i\rvert)_{\max}$		0.2651	0.1673	0.1043	0.4593	1.0000
Energy spectrum	(3,0)	0.0760	0.0313	0.0090	0.2406	1.0000
	(3,1)	0.2895	0.3819	0.4442	0.3164	1.0000
	(3,2)	0.7519	0.7975	0.7743	1.0000	0.5609
	(3,3)	0.8278	0.9355	0.9447	1.0000	0.7870
	(3,4)	0.7039	0.8297	0.6819	1.0000	0.6179
	(3,5)	0.8654	0.9538	1.0000	0.9982	0.8464
	(3,6)	0.9348	0.8206	1.0000	0.9113	0.7074
	(3,7)	0.7179	1.0000	0.7544	0.7652	0.7228

on Table 1, defect types can be identified, and the identification results are listed in Table 2.

4.2. **Defect type detection based on VAEM.** In VAEM, the velocity and amplitude of each wave are also utilized. In the spectrum extraction stage, the wavelet functions and the number of decomposition levels are adjusted according to the extraction performances. Finally, the function *db*5 and 3 levels are adopted, and then the number of each energy spectrum is 8, so the number of elements of each CEV is 10. A group of CEVs of all type defects are listed in Table 3.

To present CEVs more directly, a column chart is illustrated in Figure 7. In next stage, the number of neurons in input layer is 10 and that in output layer is 5. The parameters of the PNN are also adjusted based on the identification results, and finally identification results of this group of CEVs are listed in Table 4.

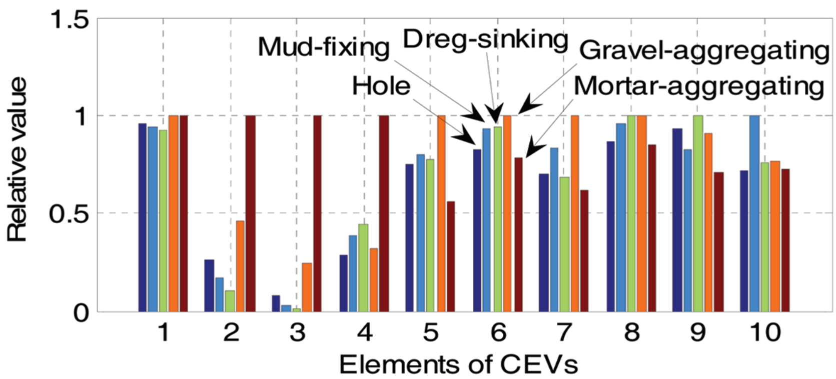

FIGURE 7. Energy column chart of CEVs

Table 4. Identification results of VAEM

Defect type	Hole	Mud -mixing	Dreg -sinking	Gravel -aggregating	Mortar -aggregating
Total	70	60	50	50	50
Identification	56	51	42	37	36
Identification rate	80%	85%	84%	74%	72%

To evaluate results, the average identification rate (AIR) is defined by Formula (11).

$$AIR = \frac{1}{\sum M_i} \sum_{i=1}^{5} IR_i \cdot M_i \tag{11}$$

where IR_i is the identification rate of the ith type defect, and M_i is the number of the sample signals of the ith type defect.

With the use of Formula (11), the AIRs of TVAM and VAEM can be calculated: $AIR_{TVAM} = 55\%$ and $AIR_{VAEM} = 79\%$, and the AIR increase is 24%. We also notice that the maximum AIRs of these two methods are 85% and 60%, and the increase is 25%. The compared results show that the accuracy and reliability of the proposed method is much better.

5. **Conclusions.** In this paper, VAEM is proposed to identify the defect types in large-diameter concrete pile detection. In this method, WPD is used to extract feature vectors and PNN to classify. To enhance the identification accuracy, the velocity and average amplitude of the signal are also acquired and used to contract corresponding CEV. Verified by the practical signals, experimental results show that the AIRs of traditional method and the proposed method are 55% and 79% respectively, and the advantage of the proposed method is obviously. However, the identification rates of some defect types are relative low, such as those of gravel-aggregating and mortar-aggregating which certainly will be the focus of our future work.

Acknowledgment. This work is partially supported by the National Natural Science Fund (11072210), the Province Science and Technology Support Project of Hebei (132758-02) and the Science and Technology Support Project of Qinhuangdao (2012021A114). The authors also gratefully acknowledge the helpful comments and suggestions of the reviewers, which have improved the presentation.

REFERENCES

[1] D. Zhu, C. Jia, S. Fan and X. Wang, Misjudgment analysis on ultrasonic transmission method for inspecting cast-in-place piles, *China Harbour Engineering*, no.4, pp.18-20, 2010.

[2] A. Yu, H. Tang, P. Liu, L. Zhang and Y. Zhou, The research on concrete filing pile defect detection by the analysis and comparison of ultrasonic transmission method and reflected wave method, *Chinese Journal of Engineering Geophysics*, vol.12, no.1, pp.111-116, 2015.

[3] B. Li, X. Chen and Z. He, A wavelet-based error estimator and an adaptive scheme for plate bending problems, *International Journal of Computational Methods*, vol.7, no.2, pp.241-259, 2010.

[4] D. H. Pandya, S. H. Upadhyay and S. P. Harsha, Fault diagnosis of rolling element bearing by using multinomial logistic regression and wavelet packet transform, *Soft Computing*, vol.18, no.2, pp.255-266, 2014.

[5] A. Banakar, M. F. Azeem and V. Kumar, Comparative study of wavelet based neural network and neuro-fuzzy systems, *International Journal of Wavelets, Multiresolution and Information Processing*, vol.5, no.6, pp.879-906, 2007.

[6] A. Tabrizi, L. Garibaldi, A. Fasana and S. Marchesiello, Early damage detection of roller bearings using wavelet packet decomposition, ensemble empirical mode decomposition and support vector machine, *Meccanica*, vol.50, no.3, pp.865-874, 2015.

[7] W. Cui, J. Wang, J. Song and J. Gao, Fault diagnosis of polymerization kettle equipment based on probabilistic neural networks, *ICIC Express Letters, Part B: Applications*, vol.6, no.7, pp.1767-1772, 2015.

[8] S. F. Jiang, C. Fu and C. Zhang, A hybrid data-fusion system using modal data and probabilistic neural network for damage detection, *Advances in Engineering Software*, vol.24, no.6, pp.368-374, 2011.